



**Fundamental limits
for light harvesting structures in the IR**

Plasmonic Innovative Sensing in the IR

www.plaisir-project.eu



OBJECTIVES OF THIS REPORT

This report has the following objectives:

- Give physical insights into the transmission efficiency of a single slit. An analytical treatment of this simple system is possible within the modal expansion formalism.
- Report on the fundamental limits found for the transmission efficiency of a slit-groove array.
- Studying possible path to achieve a disruptive impact on the detection market by improving the signal to noise ratio of detectors using the bull's eye geometry.

This deliverable is divided into two main sections:

- **Methodology.** This section briefly reviews the modal expansion method and describes the geometry of the considered systems. For the sake of completeness, we have summarized simple design rules that led to optimal light harvesting structures.
- **Main results and analysis.** This section explains the fundamental limits for the transmission efficiency of a slit-groove array and the bull's eye geometry.



METHODOLOGY

We have studied the transmittance of an opaque metal film perforated with an aperture, which size is equal to typical dimensions of standard detectors in the Mid-IR. The metal surface was corrugated in order to squeeze additional light into the aperture. Figure 1 shows a schematic representation of the system considered. Its optical response was evaluated with the modal expansion formalism under the fundamental mode approximation.

Within the modal expansion formalism, Maxwell's equations are solved self-consistently using a convenient representation for the EM fields. In both substrate and superstrate (see Figure 1), the fields are expanded into an infinite set of plane waves with both p- and s-polarizations. Inside the holes the most natural basis is a set of waveguide modes. The parallel components of the fields are matched at the metal/dielectric interface using surface impedance boundary conditions (SIBCs). Although SIBCs neglect the tunneling of EM energy between the two metal surfaces, this effect is not relevant for a metal thickness larger than a few skin depths. SIBCs are also employed at the lateral wall of the holes. After matching the fields at the interface, we arrive to a system of tight binding-like equations for the amplitude of the electric field at the hole openings.

In search for high efficiencies in the light harvesting process, we have considered the interplay between Fabry-Pérot modes of a single slit and groove cavity modes of the groove array. The following design rules should be taken into account along the optimization algorithm:

- Fabry-Pérot and groove cavity modes should be at the same spectral position.
- Ideal periodicity: $P \approx 0.9-0.95 \lambda_{\text{spp}}$, where λ_{spp} is the SPP wavelength.
- Groove depth about half the metal thickness.
- Slit-nearest groove distance $\approx 0.9 P$ (for optimal P).
- Groove width, w_g : either $w_g \approx h_g$ or $w_g \approx 4-6 h_g$, where h_g is the groove height.
- System's size: maximum for $7.5 L_{\text{spp}}$, where L_{spp} is the propagation length of the SPP in the corrugated surface.

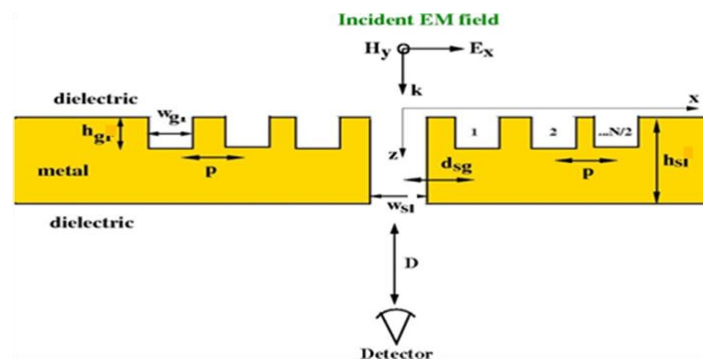


Figure 1. Schematic representation of the light harvesting structure under study

Design rules for the bull's eye geometry have been reported in Mahboub *et al.* *Opt. Express* **18**, 11292 (2010).



MAIN RESULTS AND ANALYSIS

We have identified the following fundamental limits for 1D slit-groove arrays harvesting IR radiation:

- The maximum normalized-to-slit-area transmittance for a single slit in a real metal is always lower (by $\approx 20\%$) than the corresponding one for a slit in a PEC, which is equal to $\lambda/\pi w_s$, where λ is the wavelength of the incident radiation and w_s is the slit width; see Figure 2.

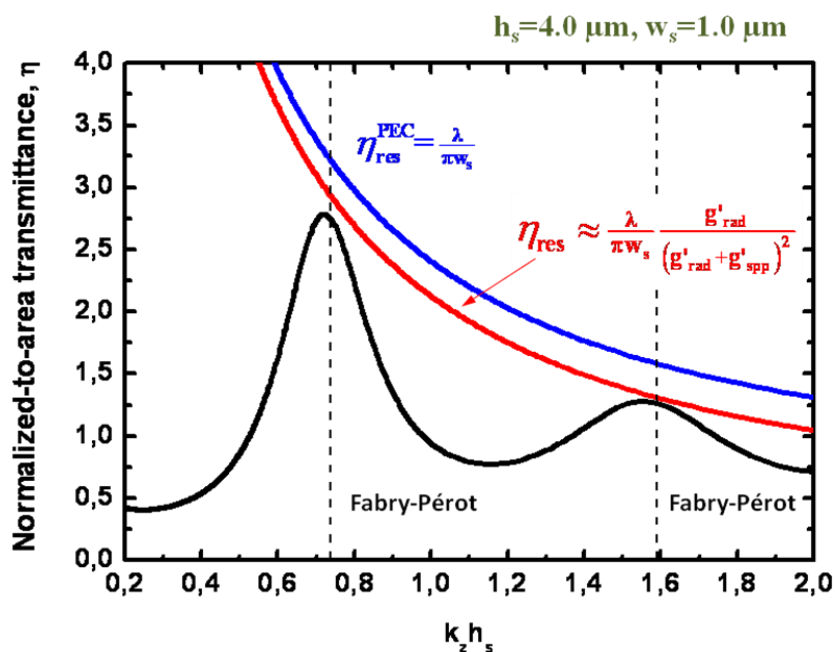


Figure 2. Normalized-to-area transmittance of a single slit (black line) as a function of $k_z h_s$, where k_z is the propagation constant of the fundamental mode in the slit and $h_s=4 \mu\text{m}$ is the metal thickness of the gold film. The slit width is $w_s=1 \mu\text{m}$. The gold film is free standing on air. The blue line represents the magnitude of the Fabry-Pérot resonance for a PEC (equal to $\lambda/\pi w_s$), while the red line gives the contribution for a real metal. The primed g s represent normalized propagators that provide the field radiated into the far-field (g'_{rad}) or scattered into surface modes (g'_{spp}).

- 10-35% of the power is scattered into surface modes at the output side of the slit, see Figure 3.

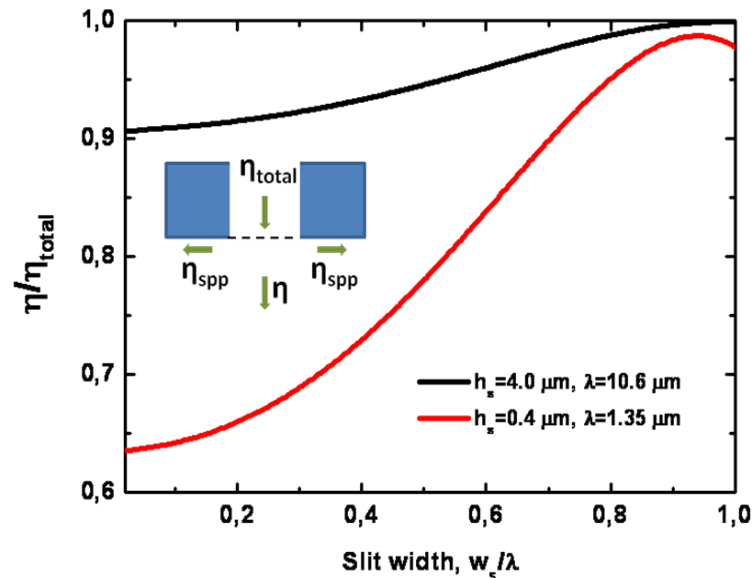


Figure 3. Ratio of the power radiated to the far field by a single slit (η) and the total power traversing the slit (η_{total}) as a function of the slit width w_s (normalized to λ). The remaining part of the power is scattered into surface modes. This ratio is almost independent of the corrugation of the illuminated surface. The black line represents a single slit at $\lambda=10.6 \mu\text{m}$ in a metal film with thickness $h_s=4.0 \mu\text{m}$, while for the red line $\lambda=10.6 \mu\text{m}$ and $h_s=0.4 \mu\text{m}$. As in Figure 2, the gold film is free standing in air.

- The maximum normalized-to-slit-area transmittance, η , of the slit-groove array does not increase with λ , c.f. Tables 1 and 2. Although metal losses are lower for increasing λ , favoring a higher transmittance, the strength of surface modes also decrease with λ , making less efficient the light harvesting process. The concomitance of lower metal losses and less-efficient harvesting of light for increasing λ produces optimal values of η which are largely independent of the wavelength. We confirm such behavior after extensive optimization of the slit-groove array for several wavelengths in the IR. Tables 1 and 2 summarize both the geometry and the efficiency of optimal slit-groove arrays for $\lambda=1.35 \mu\text{m}$ and $\lambda=10.6 \mu\text{m}$, respectively.
- A narrower spectral width is found for the slit-groove array with largest η , e.g. the spectral width is 56 nm for $\lambda=1.35 \mu\text{m}$ and 530 nm for $\lambda=10.6 \mu\text{m}$ in Tables 1 and 2.
- We find a small tolerance in groove depth and groove period, which are also the geometrical parameters most relevant in the optimization process. The tolerance is estimated by the full width at half maximum (FWHM) of η as a function of the corresponding quantity, see Tables 1 and 2.

PARAMETERS		FWHM [nm]
Metal	Gold	
Substrate	air	
Pixel size, $L=2N P$	25 μm	
Number of Grooves, N	10+10	
Slit width, w_s	100 nm	
Targeted wavelength	1350 nm	56
Groove depth, h_g	124 nm	38
Groove period, P	1258 nm	70
Groove width, w_g	114 nm	186
Slit- groove dist., d_{sg}	1199 nm	224
Metal thickness, h_s	360 nm	231
Max. normalized transmittance, η_{max}	61	

Table 1. Geometry, efficiency, and tolerance of the geometrical parameters (estimated by the FWHW) for the optimal slit-groove array at $\lambda=1.35 \mu\text{m}$.

PARAMETERS		FWHM [nm]
Metal	Gold	
Substrate	air	
Pixel size, $L=2N P$	1.99 mm	
Number of Grooves, N	10+10	
Slit width, w_s	1,00 μm	
Targeted wavelength	10.6 μm	540
Groove depth, h_g	1,23 μm	520
Groove period, P	10,1 μm	680
Groove width, w_g	1,67 μm	2190
Slit- groove dist., d_{sg}	9,24 μm	1840
Metal thickness, h_s	3,60 μm	1190
Max. normalized transmittance, η_{\max}	63	

Table 2. Geometry, efficiency, and tolerance of the geometrical parameters (estimated by the FWHW) for the optimal slit-groove array at $\lambda=10.6 \mu\text{m}$.

Other relevant figures of merit

In previous figures we have computed the transmitted power normalized to the incident power on the slit. It is also worth to normalize the transmitted power to the power incident on the whole slit-groove array, in order to obtain the total transmission, T . It is reported in Figure 4 for the optimal structure of Table 2. We find in Figure 4 that 30% of the incident light is transmitted through the optimal structure.

The figure of merit $T\eta^{1/2}$ is also defined within the project in order to account for the S/N ratio. It reaches a maximum value of 2.5 for the optimal structure, Figure 5.

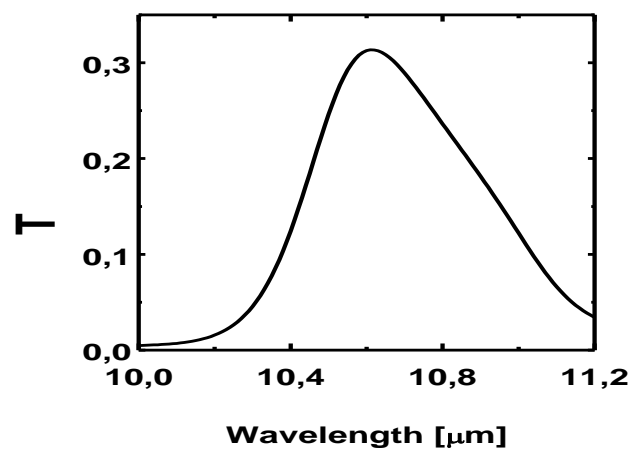


Figure 4. Total transmission as a function of the wavelength for the optimal structure of Table 1

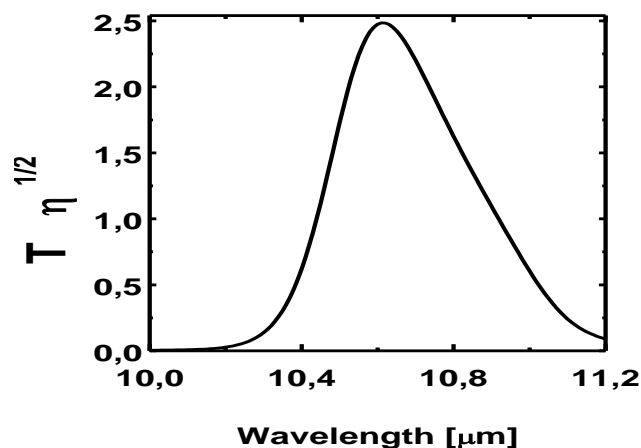


Figure 5. The figure of merit $T\eta^{1/2}$ as a function of the wavelength for the optimal structure of Table 1

Figures of merit for the bull's eye geometry

The bull's eye (BE) geometry deserves a separate discussion. In the light harvesting process, a BE is more efficient than a slit-groove array. We observe in Figure 6 that an annular hole flanked by only 5 grooves has a normalized-to-area transmittance $\eta=304$ at $\lambda=10.6 \mu\text{m}$ (the geometrical parameters are described in Table 3). A lower $\eta=63$ was obtained for the slit-groove array with twice the number of grooves (10 grooves at each side of the slit) at the same wavelength, see Table 2. Despite the large difference in this concentration factor, the BE has lower S/N figures of merit ($T\eta^{1/2}$) than the SGA (c.f. Figure 5 and Figure 7). The reason for that behavior is that the fraction of the BE area occupied by the annular hole is smaller than the fraction occupied by the slit in the 1D SGA.

Although the BE geometry is ideally suited for having large η , in principle, both T and the S/N FOM can also be tuned: increasing the number of grooves, N , additional light is squeezed into the central hole of the BE, enhancing η but reducing T . On the other hand, for smaller N , the total area of the system is smaller, thus increasing T at the price of having less-efficient light harvesting processes; so, lower values of η are obtained.

In the search for an optimal S/N FOM, the BE should be therefore optimized not only as a function of its geometrical parameters, but also as a function of N . Consequently, the computation cost of the optimization process is higher. This procedure is not always useful for practical applications of the BE because typical detectors are fabricated for given pixel size, so we have a given constraint in the number of grooves that can be considered in the simulations.

In the present report, we have optimized a homogeneous groove array, i.e. all the grooves have the same depth and width. A further enhancement can be obtained by optimizing the geometry of each individual groove scanning the parameter space with help of the conjugate gradient method. An enhancement of 2, with respect to the homogeneous system, is typically obtained with this optimization method. That would imply a S/N FOM $2^{3/2} \approx 2.8$ times larger than for the homogeneous BE.



CONCLUSIONS

The normalized-to-slit-area transmittance of the slit-groove array could reach the value $\eta \approx 60$, independently of the wavelength of the incident IR radiation. The price to pay for such high intensity is a narrow spectral width and small tolerances in both groove depth and groove period. η could be even larger ($\eta \approx 300$) for a BE with an annular hole, though having smaller total transmission T and S/N FOM.

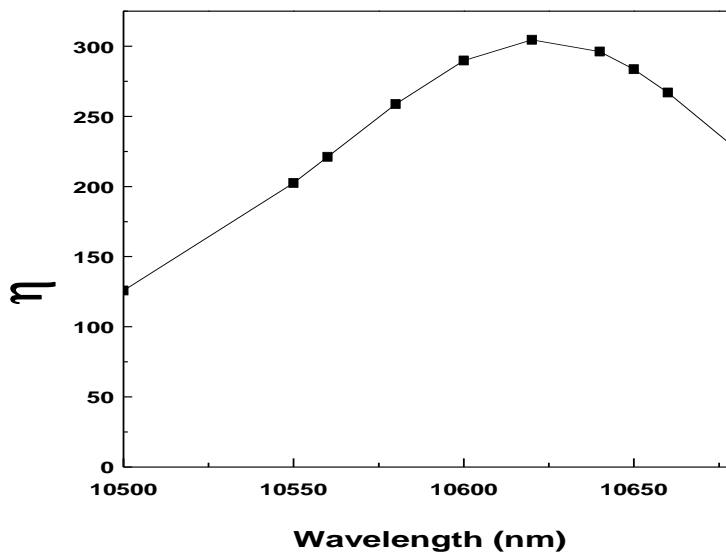


Figure 6. Normalized to hole-area transmittance as a function of the wavelength for the optimal structure of Table 3.

PARAMETERS	
	Gold
Substrate	air
Number of Grooves, N	5
Inner annular-hole radius, r_{in}	1,6 μm
Outer annular-hole radius, r_{out}	1,8 μm
Targeted wavelength	10.6 μm
Groove depth, h_g	2,1 μm
Groove period, P	9,8 μm
Groove width, w_g	0,6 μm
Slit- groove dist., d_{sg}	9,7 μm
Metal thickness, h_s	4,0 μm
Max. normalized transmittance, η_{max}	304

Table 3. Geometrical parameters of a bull's eye structure with an annular hole optimized at $\lambda=10.6 \mu\text{m}$

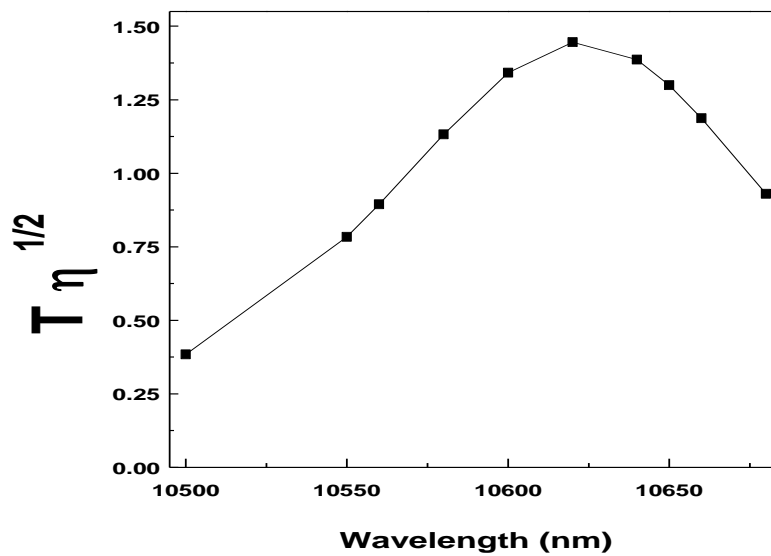


Figure 7. S/N figure of merit, $T\eta^{1/2}$, as a function of the wavelength for the optimal structure of Table 3

GLOSSARY

Acronym	Signification
IR	Infra-red
UV	Ultra-violet
NIL	Nano imprint lithography
FIB	Focused Ion Beam Milling
InGaAs	Indium Gallium Arsenide
MCT	Mercury Cadmium Telluride
InGaAs	Indium Gallium Arsenide
ME	Modal expansion
SIBCs	Surface impedance boundary conditions
PEC	Perfect electric conductor
FDTD	Finite difference time domain
LHS	Light harvesting structure
SGA	Slit-groove array
BE	Bull's eye structure
fom	Figure of merit
S/N	Signal to noise